Low-temperature spin-wave excitations in nickel, by neutron triple-axis spectroscopy

P. W. Mitchell
Department of Physics, University of Edinburgh, Mayfield Road, Edinburgh EH9 3JZ, United Kingdom

D. McK. Paul*
Institut Laue-Langevin, 156 X, Grenoble, France
(Received 25 January 1985)

Measurements have been made of the low-energy spin waves ($\nu < 3$ THz) in nickel at temperatures from liquid-helium temperatures up to room temperature. New data-analysis procedures, involving resolution convolutions on an International Computers Ltd. Distributed Array Processor (DAP) computer, have allowed the separation of the spin wave from phonon cross sections. The values deduced for the spin-wave stiffness ($D = 96 \pm 5$ THz Å^2 at $T = 1.5$ K and $D = 95 \pm 3$ THz Å^2 at $T = 295$ K) are seen to be in agreement with some previous estimates and differences from others are explained. In particular, the low-temperature value agrees with the magnetization results, showing that the spin waves can account for all of the observed magnetization changes.

I. INTRODUCTION

The ground-state properties of ferromagnetic nickel are now considered to be well understood.[1] Detailed band-structure calculations have been performed[2] using the local-spin-density approximation to the spin-density-functional theory, and these give good agreement with measured values of the ground-state magnetization, but overestimate the band splitting.[1,3] The uncertainties which remain in the theory of the ground state are overshadowed by the problems involved in constructing a theory of the thermodynamic properties of nickel.

The first step in such a procedure is to calculate the elementary excitations of the system, and a first-principles calculation, carried out by Cooke *et al.*[4] for a realistic band structure, within the random-phase approximation (RPA which excludes electron correlation effects), has produced a remarkably good picture for the magnetic excitations in nickel, even to the extent of predicting an optic mode which has subsequently been observed.[5] Callaway *et al.*[6] also extended their band-structure calculations to include the low-lying magnetic excitations and have calculated the zero-temperature spin-wave stiffness (coefficient of the quadratic term for the energy as a function of wave vector). Such calculations, however, are limited by the accuracy of the ground states they use, so that, for example, Callaway *et al.* expect their spin-wave stiffness to be an overestimate, as their band splitting is known to be.[3]

Going on from the elementary excitations to a theory capable of dealing with the reduction of the magnetization as the temperature is raised (incorporating the renormalization of the excitation energies) and the destruction of the long-range order at the Curie temperature T_C and the magnetic state above T_C is not yet possible from first principles, although much current work, both experimental and theoretical, is devoted to this last area.[7]

Many attempts have been made, however, in a semi-empirical way, to describe the temperature dependence of the magnetization in terms of the elementary and renormalized excitations.[9–11] The basic aim of much of this study has been to assess whether the reduction of the magnetization can be accounted for solely in terms of the spin-wave excitations, or whether some other mechanism is involved. The most popular candidate has been the single-particle or Stoner excitations, which are excited quasiparticles and holes of opposite spin. In Stoner theory, in its original form, these are the only low-lying magnetic excitations available to the system, and they lead to a temperature dependence of the magnetization which may be quadratic in temperature (T^2), exponential [$T^{3/2}\exp(-\Theta/T)$], or like $T^{3/2}$, depending on whether the ferromagnet is weak (*d*-like electron states of both polarizations present at the Fermi surface), strong (*d*-like electron states of only one polarization at the Fermi surface), or at the transition from weak to strong ferromagnetism.[10,12]

The similarity of the temperature dependence of the magnetization due to spin-wave excitations, where the leading term is $T^{3/2}$ in simple cases, means that even extremely precise magnetization data are unable to separate unambiguously contributions from collective (spin-wave) and single-particle excitations.[1,9,11] One way of making the separation is to take values of the spin-wave stiffness from neutron inelastic scattering measurements and compute the magnetization change this would cause and to assign the remaining magnetization change to the Stoner excitations. When Aldred[9] pursued this line, he found that either the quadratic or the exponential Stoner term could account for the difference, but Riedi,[10] with more precise data, concluded that the T^2 term was the best description of the data, implying that the nickel is a weak ferromagnet or at least is close to being so (i.e., a very small energy gap separates the top of the full majority spin band and the Fermi level).

This problem, which has acquired the name "the hid-

den excitation problem" (meaning that there are excitations contributing to the thermodynamic properties which are not observed in neutron scattering experiments), became very much more acute in the light of various de Haas—van Alphen studies of the Fermi surface of nickel over the last decade.[13,14,1] These show first that nickel is a strong ferromagnet, in the sense that there is only one spin state at the Fermi level which is of predominantly d character (although there is also an s-p-like state with majority carriers at the Fermi level). Second, they show that the orbit areas do not change, up to 20 K, nearly enough to explain the observed "magnetization deficiency" in terms of single-particle excitations. Thus we are left with a discrepancy between the magnetization change predicted from a knowledge of the spin-wave dispersion relation as measured by neutron inelastic scattering and the measured magnetization change as a function of temperature.

The great weakness of the argument is that, for reasons of considerable technical difficulty, the neutron inelastic scattering measurements have not been made in the most convincing way. The principal problem is that the magnon energies of interest, say, in determining the magnetization change up to 20 K, are in a region where the magnon and phonon energies are very similar. There are three neutron scattering techniques which have been used to make measurements of the low-energy spin waves. These are the diffraction method, the small-angle scattering method, and triple-axis spectroscopy. A review of the three methods is given by Shirane *et al.*[15] In principle, the triple-axis method is superior to the others because it measures the spin-wave energies directly, and therefore there is no need to know the functional form of the dispersion relation in advance. It may be deduced from the measurements. There seem to be systematic errors which can creep into the other two methods which are hard to quantify. For example, applied magnetic fields are required for both techniques, and this introduces an energy gap at zero wave vector which complicates the analysis and may also modify the actual dispersion relation parameters. By contrast, the triple-axis method in its simplest form works in zero applied field, when the gap corrections are due to magnetocrystalline anisotropy and magnetic interaction effects and are generally quite small. For these reasons, if there is a difference detected between the results of different measurements of the excitation energies at given wave vectors, the triple-axis results are to be preferred.

However, there are three pronounced difficulties with the triple-axis technique concerning the low-energy spin waves in nickel at low temperatures. The first problem is that, because the spin-wave energies change very rapidly with wave vector, good resolution must be employed to ensure that the resolution function is not averaging over too large a range of wave vectors at once. Second, the phonon scattering, even in separated isotope ^{60}Ni, becomes comparable in intensity with, and even stronger than, the spin-wave scattering, because of the term in the phonon cross section proportional to the reciprocal of the energy transfer. Finally, when the resolution of the spectrometer is good enough to avoid the first problem, and to mitigate the second (by allowing separation of the magnon and phonons by line-shape differences), the scattering intensity in the spin waves is extremely low, especially at low temperatures, where the population factor becomes small. Thus the neutron source strength dictates the limit to the resolution.

For these reasons, all previous measurements of the spin-wave spectrum at room temperature and below using triple-axis spectroscopy have concentrated on the region where the magnon energies are well above the phonon energies (the magnon and longitudinal phonon cross at about 1 THz).[16–20] Furthermore, the only published measurement (at room temperature only) below the phonons[17] shows that there are considerable deviations from the quadratic dispersion relation, even at 2.5 THz. This means that it is certain at room temperature, and probable at lower temperatures, that extrapolation from the higher-energy data to low energies will overestimate the spin-wave stiffness D. Thus we see that there are no published triple-axis measurements which can be relied upon to estimate D at low temperatures, for comparison with the magnetization data. The values of D used by Aldred[9] and Riedi[10] are not taken from neutron scattering data in the appropriate energy range (less than 0.5 THz for Riedi's data up to 20 K), but from much-higher-energy spin waves, which are not, in fact, populated significantly in the temperature range of comparison.

The change that has enabled us to make progress on this difficult problem is the development of a computer program (SHAMGAR) to run on an International Computers Ltd. Distributed Array Processor (DAP) computer, which performs the necessary resolution-convolution integrals sufficiently quickly to allow rapid simultaneous fitting of a model scattering law to many scans of an experimental triple-axis data set.[21] Phonon and magnon separation can be achieved reliably by demanding continuity of the various cross sections through all the scans.

In Sec. II the experimental procedure will be described. Section III presents the results of the present measurements and compares them with previous measurements and theoretical predictions. Section IV discusses the implications of the results.

II. EXPERIMENTAL PROCEDURE

A. Spectrometer

The experiment was carried out on the triple-axis spectrometer IN3, installed on a thermal neutron guide tube at the Institute Laue-Langevin (ILL), Grenoble. Pyrolytic graphite was used as both monochromator and analyzer, and a pyrolytic graphite filter was used between the sample and analyzer to filter out order contamination. Various horizontal collimation conditions, spectrometer configurations, scattered wave vectors, and monochromator and analyzer reflections were employed to optimize the resolution conditions and counting rates at different energy transfers.

The magnon measurements were all carried out in the vicinity of the (111) reciprocal-lattice point and mostly with the (004) reflections at both monochromator and

analyzer, using a fixed scattered wave vector k_F of 2.662 Å^{-1}, corresponding to the use of the filter to eliminate $2k_F$ and $3k_F$ contamination. Horizontal collimation was typically 20′(guide)-30′-30′-40′, although 20′-30′-20′-30′ was used at lower-energy transfers to improve the resolution. Some of the higher-energy-transfer scans were performed using the (002) reflections from the analyzer or both monochromator and analyzer, and various senses of scattering at the sample and analyzer were employed largely as a result of physical constraint [e.g., at high incident energies (small monochromator take-off angles), scattering to the left of the sample is not possible because the guide prevents the analyzer from being used on that side]. Phonon measurements were made in the vicinity of the (222) reciprocal-lattice point, where the phonon cross section is larger and the magnon cross section smaller than near the (111).

The various conditions were employed after optimization of the parameters using the computer program SHAMGAR (Ref. 21) to generate the form of the scattering by convolution of a model scattering law with the full resolution function of the instrument.[22] The program is described in further detail in Sec. II D below.

B. Crystal

The single crystal used in the experiment was on loan from Brookhaven National Laboratory and was the ^{60}Ni isotope crystal used by Minkiewicz *et al.*[16] The mosaic structure of the crystal was examined and found to be nearly Gaussian, with a full width at half maximum of 20 minutes of arc. This was incorporated into the instrumental resolution calculation following Werner and Pynn.[23]

C. Cryostat

The cryostat used was a standard ILL "orange" cryostat, employing flowing liquid ^{4}He to cool a copper block anchored to the heat shield nearest the sample. The cryostat is top loading with a rhodium-iron resistance thermometer mounted in good thermal contact with the sample holder, to which the crystal was fixed using Kwikfill paste. The sample temperature was variable between 1.5 and 300 K. Data were taken at 1.5 K for the measurement of the spin-wave energies at low temperature, 97 K as an intermediate temperature, and 295 K for comparison with previous measurements which were made using different techniques.

D. Data-analysis procedure

As described above (Sec. I), the data-analysis procedure is an important part of this experiment. However, it represents not a new approach to the problem, but simply a very much faster method. The intensity observed in the triple-axis measurement is taken to be the convolution of the resolution function and the model cross section [Ref. 22, Eq. (10)]. The resolution function is computed in the Gaussian approximation of Cooper and Nathans for each point of each experimental scan, and the scattering intensity is deduced by four-dimensional numerical convolution of this function with a scattering law representing the phonon branches and a spin-wave branch, with adjustable parameters to represent the phonon speeds and weights, the weights of the spin-wave scattering, and the energy dispersion relation of the spin waves. The magnetic form factor is accounted for by a term $\exp(-\alpha Q^2)$ with $\alpha=0.066$ Å^2. The spin-wave energies are represented by a function of the form

$$\epsilon=\epsilon_0+D\,|\,q\,|^2+E\,|\,q\,|^4 . \tag{1}$$

A background term is also added to the calculated intensity. Thus a complete set of data is generated corresponding to all of the experimental scans chosen, and the generated curve is fitted to the data by a weighted least-squares procedure.

Because of the architecture of the DAP computer on which the program runs (64×64 array of processor units), it is convenient, and sufficiently accurate, to perform the convolution integral on a grid of $16\times16\times16$ points which is set up in reciprocal space in the frame in which the resolution function, projected down the energy axis, is diagonal. The energy integral is performed analytically for each point thus selected in reciprocal space, using the δ function appearing in the phonon and magnon cross sections. The range of integration in each dimension is chosen such that all contributions from parts of the resolution function less than $\exp(-3)$ of the maximum are set to zero.

The time taken for an interactive session analyzing six scans each of 20 points, allowing five parameters to vary in the fit, with one spin wave and one phonon branch included, was typically ten minutes, varying slightly with the weight of use on the Edinburgh EMAS system. This is sufficiently fast for a number of different ways of analyzing the data to be tried out and to select appropriate sets of scans to determine ϵ_0, D, and E at the various temperatures.

III. RESULTS

Data were taken in the nominal energy ranges $0.25<\nu<3$ THz at $T=1.5$ and 295 K and $0.5<\nu<1.25$ THz at $T=97$ K. The phonon velocities were fixed at their measured values and the spin-wave energies deduced from the fitting procedure described above.

The results for the parameters ϵ_0, D, and E at $T=1.5$ and 295 K and D at $T=97$ K are shown in Table I. Because of the nature of the data, not much information is contained in one scan. We therefore illustrate the results in Fig. 1, showing six scans at $T=1.5$ K (four constant-energy scans and two constant-wave-vector scans), with the measured data points, the fitted simulated intensities, the background function (flat background plus phonon scattering), and the spin-wave contribution to the total scattering. We emphasize that, although this data is not very good statistically, point for point, largely because at these low temperatures the scattering intensities are very low, yet the required information may be obtained from it. At higher temperatures, the data quality improves because of the increase in the population factor in the intensity, and this is reflected in smaller error estimates for the fitted parameters (Table I). The agreement is statistically

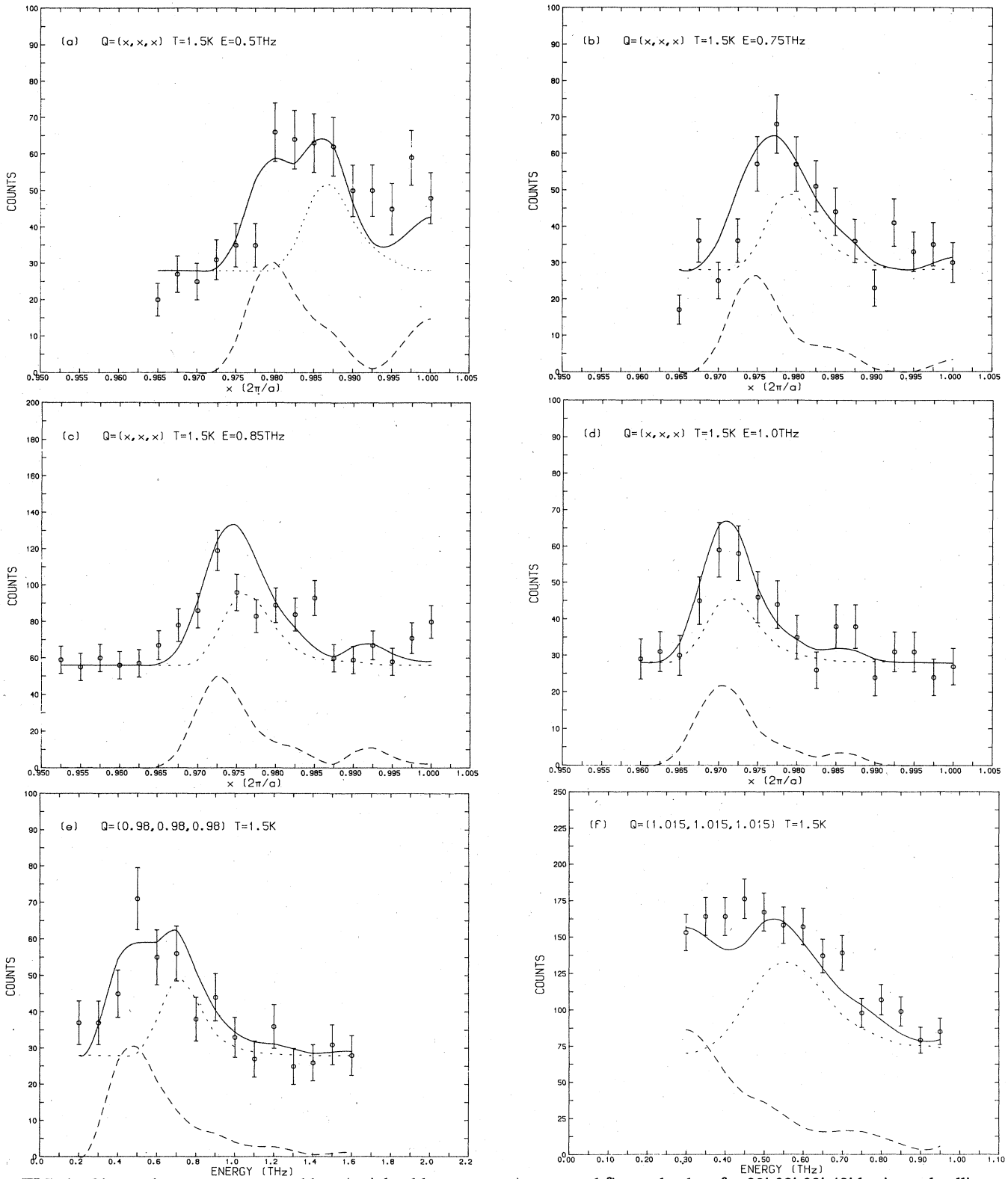

FIG. 1. Observed neutron counts and best (weighted least-squares) computed fits to the data for 20′-30′-30′-40′ horizontal collimation, PG(004)-PG(004) (PG denotes pyrolytic graphite). The solid line is the calculated curve, the dashed curve is the spin-wave contribution, and the dotted curve is the background and phonon contributions. There were approximately 10 000 monitor counts per minute, varying slightly as k_I was changed. Monitor counts were 300 000 per point, except for (c) 600 000 and (f) 750 000. The oscillations in the calculated spin-wave cross section are due to the coarseness of the mesh in the integration procedure, but are not important compared to the data errors.

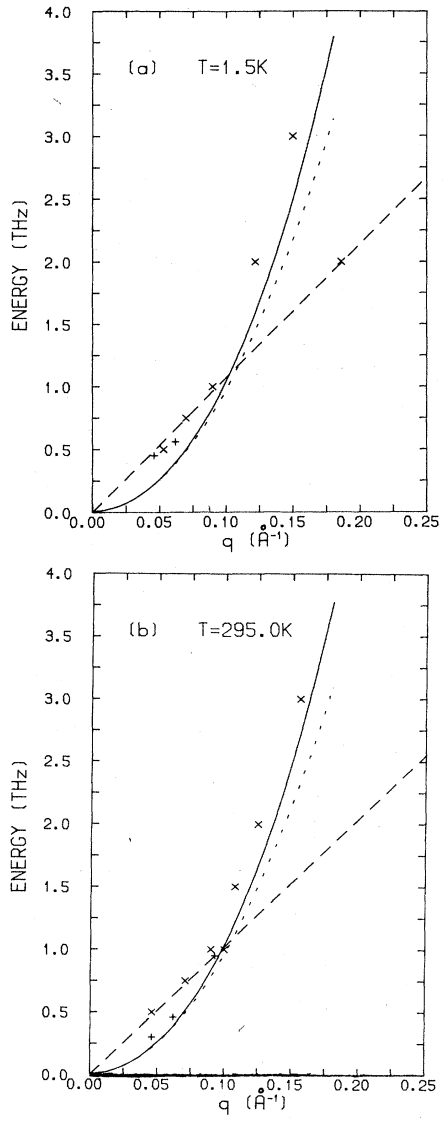

FIG. 2. Reconstructed spin-wave dispersion relation for nickel at (a) $T=1.5$ K and (b) $T=295$ K. Dashed line is longitudinal acoustic phonon; dotted line is spin-wave energy without the quartic term; +, peaks observed in constant-wave-vector scans; ×, peaks observed in constant-energy scans. These figures show first the importance of making the resolution corrections carefully, as the significant shifts from the observed peaks to the calculated dispersion relations show, and second the importance of including the quartic term to account for data above 1.0 THz, or conversely, the impossibility of deducing D from measurements at energies higher than 1.0 THz alone.

satisfactory in all cases. Figure 2 shows the spin-wave dispersion relation reconstructed from the parameters [Eq. (1)].

The present results are compared in Table II with results obtained by other methods and earlier triple-axis measurements. Two first-principles theoretical estimates are also included in the table. Two important features may be seen from this comparison. First, the present value for the spin-wave stiffness at low temperature is in good agreement with other measurements at low temperatures (magnetization and hyperfine field). There are no other values derived from low-temperature neutron scattering experiments at all to our knowledge. The closest is the value extrapolated from higher temperatures estimated by the small-angle cutoff method by Hatherly *et al.*[25] Previous triple-axis measurements at low temperatures have involved extrapolation from high energies and give rise to a much larger value of D.

TABLE I. Results of the present measurement. For the definitions of ϵ_0, D, and E, see Eq. (1). Numbers in parentheses are estimated errors as derived from the fitting procedure (the change in the parameter which if made, and all the other parameters adjusted to minimize χ^2, would increase χ^2 by one standard deviation of the χ^2 distribution).

T (K)	ϵ_0 (THz)	D (THz Å^2)	E (THz Å^4)
1.5	0.015(10)	96(5)	630(50)
97		96(4)	
295	0.015(6)	95(3)	655(35)

Second, the room-temperature value of the stiffness is the same as the low-temperature value, to within the estimated error. This stands in agreement with the estimate of Minkiewicz *et al.*[16] from their room-temperature data, but in stark contrast to the values derived from magnetization and hyperfine field data. The agreement with other neutron techniques (small-angle scattering and diffraction method) is good for the stiffness, but note that the tendency of the diffraction method to underestimate the spin-wave energy at larger wave vectors[15,16] gives rise to the wrong sign for the quartic term E. The other triple-axis measurements give a very much lower estimate for the stiffness at room temperature than at low temperature, but they still give larger values than the present result.

IV. DISCUSSION AND CONCLUSIONS

The present results provide confirmation that, at least at low temperatures, there are no hidden excitations in nickel. That is to say, the decrease in the magnetization can be accounted for completely by the thermal population of the spin waves. This, along with the Fermi surface measurements of Lonzarich,[1] confirms that thermal population of the Stoner modes is insignificant at low temperatures.

Discrepancies between these results and previous triple-axis estimates of the stiffness at low temperatures may be understood in terms of the large deviations from the initial quadratic dispersion relation, even at quite small wave vectors. This is in agreement with the measurements of Minkiewicz *et al.*[16] at room temperature and confirms that similar deviations are also important at low temperatures.

The estimated renormalization of the stiffness up to room temperature is less than the estimated errors and suggests that the fractional change in the stiffness is no greater (it may even be less) than the fractional change in the magnetization over the same temperature range ($\sim 6\%$).

TABLE II. Comparison with previous results. Values of D in THz Å^2. Values in square brackets are for E in THz Å^4. Numbers in parentheses are estimated errors, as in Table I.

Technique	Reference	$T<5$ K	$T=295$ K
Neutron	16		97
triple-axis	17		105
	18	134	
	20	127(4)	111(4)
	19	133	102
	19	143[−98]	122[−120]
	This work	96(5)[630(50)]	95(3)[655(35)]
Neutron	24		99(3)
small-angle	25	102(7)[a]	
scattering			
Neutron	26		90(5)
diffraction	26		94[−96]
method			
Magnetization	8	95.3(1.7)	
	27	93(9)	
	9	95.5(1.2)	
	9	87.5(0.2)	65.5
Hyperfine field	10	96.1(1.0)	62.9
Theory	4	203	
	6	136	

[a]Not measured at low T, but extrapolated from high T.

Theoretical first-principles estimates of the ground-state spin-wave stiffness have been overestimates. That of Callaway *et al.*[6] was expected to be, as their band-structure calculation overestimated the exchange splitting energy, but that of Cooke *et al.*[4] appears to be out by a factor of 2. [The value we quote is deduced from their Fig. 8, at the smallest wave vector (0.0625,0,0).] The same calculation gives very good agreement with data at higher energies, but can perhaps be expected to be less reliable at low energies, since the energies involved in the band-structure calculation are typically three orders of magnitude larger than the relevant spin-wave energies. (This result may also be affected by the size of the k mesh used in the calculations, which is possibly not fine enough to make reliable deductions from such small q values.)

Thin film resonance has also been used to estimate spin-wave parameters in nickel[28] but these results have not been included in the detailed comparison above because there seem to be severe problems in the interpretation of such data, with values of D at room temperature varying from 39 to 112 THz Å^2 from different experiments (Ref. 28 and references therein).

The room-temperature values of D estimated from magnetization and hyperfine field measurements are in severe disagreement with the present results, but since they are averaging over a wide energy range, at that temperature, we believe the neutron value, which is consistent among all three neutron techniques used at room temperature, is to be preferred.

ACKNOWLEDGMENTS

This work was funded by the Science and Engineering Research Council. We are grateful to G. Shirane of Brookhaven National Laboratory for the loan of the crystal and to P. C. Riedi and G. G. Lonzarich for stimulating discussions.

*Present address: Department of Physics, University of Warwick, U.K.

[1]G. G. Lonzarich, in *Electrons at the Fermi Surface,* edited by M. Springford (Cambridge University Press, Cambridge, U.K., 1980), p. 225.

[2]J. Callaway and C. S. Wang, Phys. Rev. B **16**, 2095 (1977).

[3]C. S. Wang and J. Callaway, Phys. Rev. B **15**, 298 (1977).

[4]J. R. Cooke, J. W. Lynn, and H. L. Davis, Phys. Rev. B **21**, 4118 (1980).

[5]H. A. Mook and D. Tocchetti, Phys. Rev. Lett. **43**, 2029 (1979); H. A. Mook and D. McK. Paul, *ibid.* **54**, 227 (1985).

[6]J. Callaway, C. S. Wang, and D. G. Laurent, Phys. Rev. B **24**, 6491 (1981).

[7]For example, O. Steinsvoll, C. F. Majkrzak, G. Shirane, and J.

Wicksted, Phys. Rev. B **30**, 2377 (1984), and references therein; P. J. Brown, H. Capellmann, J. Deportes, D. Givord, and K. R. A. Ziebeck, J. Magn. Magn. Mater. **31-34**, 295 (1983); D. M. Edwards, *ibid.* **36**, 213 (1983); V. Korenman, J. Murray, and R. E. Prange, Phys. Rev. B **16**, 4032 (1977).

[8]B. E. Argyle, S. H. Charap, and E. W. Pugh, Phys. Rev. **132**, 2051 (1963).

[9]A. T. Aldred, Phys. Rev. B **11**, 2597 (1975).

[10]P. C. Riedi, Physica **91B**, 43 (1977).

[11]P. C. Riedi, Phys. Rev. B **20**, 2203 (1979).

[12]E. C. Stoner, Proc. R. Soc. London, Ser. A **165**, 372 (1938).

[13]A. V. Gold, J. Low Temp. Phys. **16**, 3 (1974).

[14]N. Cooper and G. G. Lonzarich (unpublished).

[15]G. Shirane, V. J. Minkiewicz, and R. Nathans, J. Appl. Phys. **39**, 383 (1968).

[16]V. J. Minkiewicz, M. F. Collins, R. Nathans, and G. Shirane, Phys. Rev. **182**, 624 (1969).

[17]H. A. Mook, R. M. Nicklow, E. D. Thompson, and M. K. Wilkinson, J. Appl. Phys. **40**, 1450 (1969).

[18]H. A. Mook, J. W. Lynn, and R. M. Nicklow, Phys. Rev. Lett. **30**, 556 (1973).

[19]J. W. Lynn and H. A. Mook, Phys. Rev. B **23**, 198 (1981).

[20]M. Hennion, B. Hennion, A. Castets, and D. Tocchetti, Solid State Commun. **17**, 899 (1975).

[21]P. W. Mitchell and M. T. Dove, J. Appl. Cryst. (to be published).

[22]M. J. Cooper and R. Nathans, Acta Crystallogr. **23**, 357 (1967).

[23]S. A. Werner and R. Pynn, J. Appl. Phys. **42**, 4736 (1971).

[24]M. W. Stringfellow, J. Phys. C **1**, 950 (1968).

[25]M. Hatherly, K. Hirakawa, R. D. Lowde, J. F. Mallett, M. W. Stringfellow, and B. H. Torrie, Proc. Phys. Soc. London **84**, 55 (1964).

[26]S. J. Pickart, H. A. Alperin, V. J. Minkiewicz, R. Nathans, G. Shirane, and O. Steinsvoll, Phys. Rev. **156**, 623 (1967).

[27]R. Kaul and E. D. Thompson, J. Appl. Phys. **40**, 1383 (1969).

[28]D. P. Mitra and J. S. S. Whiting, J. Phys. F **8**, 2401 (1978).